Elaboration and electrochemical characterization of new fused heterocyclic systems as organic electrodes

S. Roudani,[1] R. Er-raqioui,[1]* R. Maallah,[2] R. El Ajlaoui,[3]* A. Chtaini,[2] S. Abouricha,[1] E.M. Rakib[1,4] and B. Hammouti[5,6]

[1]Laboratory of Molecular Chemistry Materials and Catalysis, Faculty of Sciences and Technics Sultan Moulay Slimane University, v Med V, BP 591, Beni-Mellal 23000, Morocco

[2]Molecular Electrochemistry and Inorganic Materials Team, Sultan Moulay Slimane University, Beni Mellal Faculty of Science and Technology, Morocco

[3]Biotechnology, Materials and Environment team, Faculty of the Sciences, IBN ZOHR University, Agadir, Morocco

[4]Higher School of Technology Director (EST-FBS), EST-Fkih Ben Saleh, University of Sultan Moulay Slimane (USMS), Beni-Mellal 23000, Morocco

[5] Euro-Mediterranean University of Fes, P.O. Box 15, 30070 Fez, Morocco

[6]Laboratory of Industrial Engineering, Energy and The Environment (LI3E) SUPMTI Rabat, Morocco

*E-mail: *r.elajlaoui@yahoo.fr; **hammoutib@gmail.com*

Abstract

In this study, we created paste electrodes by blending graphite carbon and natural phosphate, with modifications using organic molecules. The objective of This study aims to create a streamlined method for characterizing specific organic products, providing a faster and simpler alternative to existing techniques. Cyclic voltammetry makes it possible to separate the properties of organic products, Through the emergence of distinct oxidation and reduction peaks. The existence of NO_2 groups within the backbone of organic molecule **A** is manifested by the disappearance of the 1 V oxidation peak (P2), and its replacement by a reduction peak around approximately –0.5 V (P5). These electrodes were also characterized by the hydrogen peroxide reduction reaction, which showed that the CPE-NP-molecule **A** electrode has a very high activity towards this reaction; whereas, the second electrode CPE-NP-molecule **B**, does not promote this reduction. In the same way the antioxidant power of the two molecules has been deduced, we find that molecule **A** has a remarkable antioxidant power compared to that of molecule **B**.

Received: November 30, 2023. Published: January 14, 2024 doi: 10.17675/2305-6894-2024-13-1-5

Keywords: *organic electrodes, cyclic voltammetry, EIS, anti-oxidant power.*

1. Introduction

In the recent past, Electrochemical sensors have found extensive use owing to their benefits, including their remarkable sensitivity, Swift reaction times, ease of use, affordability, downsized form factors, and in recent years, the field of automated systems [1–3] has witnessed significant expansion. Particularly notable is the robust growth in research endeavors aimed at advancing electrochemical sensors for the detection of heavy metals. This surge is driven by continuous innovations in materials and manufacturing techniques [4, 5]. Notably, there has been a marked rise in the adoption of depositing organic layers onto surfaces in the construction of electrochemical sensors. This increased adoption can be attributed to their unique qualities, including a substantial surface area and strong adsorption capabilities. Furthermore, recent studies have reported the utilization of various carbon paste modifiers in the realm of electrochemical stripping analysis for the detection of heavy metals. More recently, approaches based on radical mechanisms have emerged to modify carbon surfaces by attaching organic species covalently [6, 7]. For analytical purposes like heavy metal electroanalysis, the electro functionalization of carbon paste surfaces is achieved through the application of mono or multilayers deposited onto them [8].

2. Experimental Part

2.1. Electrochemical selenium-catalyzed reaction

Selenium catalysis has emerged as a viable alternative to various transition metal catalysts due to its excellent functional group compatibility, mild reaction conditions, and remarkable selectivity [5]. Since Sharpless' pioneering work in 1979 that demonstrated the organoselenium-catalyzed allylic chlorination of olefins with *N*-chlorosuccinimide, the field of organoselenium catalysis has undergone significant development, yielding diverse and reliable synthetic strategies [9].

2.2. Electrochemically mediated coupling of aromatic/heterocyclic rings with selenides:

From the point of view of drug design, the combination of (hetero)arene and organoselenium groups has been successfully applied in various drug candidates. Therefore, the building of C–Se bonds on (hetero)arenes has become a research hotspot in the last decade. In 2018, Sun's group introduced an efficient electrochemical strategy for the direct C–H selenation of various indole derivatives and imidazo[1,2-*a*]pyridines [10].

2.3. Equipment

Electrochemical analyses were conducted using a Volta lab potentiostat (Model PGSTAT 100, Eco Chemie BV, Utrecht, The Netherlands), with operational control managed via the Volta lab Master 4 software. In this study, a saturated calomel electrode (SCE) was employed as the reference electrode (RE), while a platinum plate served as the counter electrode (CE).

2.4. Preparation of CPE-PN/ molecules

The modified carbon paste electrode was created through a precise blending process, which involved thorough mixing of natural phosphate, graphite powder, and the organic molecule powder within a small mortar until a uniform paste consistency was attained. Following this, the paste was manually inserted into the cylindrical cavity of the electrode body (with a geometric surface area of approximately 0.1256 cm^2). Electrical connectivity was established using a carbon bar. The natural phosphate utilized in this study originates from the Khouribga region (Morocco) [11–13].

3. Results and Discussion

3.1. Carbon paste electrode altered using natural phosphate

3.1.2. Characterization of natural phosphate

The surface morphology of natural phosphate underwent examination using scanning electron microscopy, as illustrated in Figure 1. Following calcination at 900°C for one hour and subsequent washing with distilled water, aimed at eliminating organic impurities, we obtained compact particles within the examined fractions, ranging from 100 to 400 μm, and these particles are rich in phosphate content [13]. The processed natural phosphate exhibited the following chemical composition: CaO (54.12%), P_2O_5 (34.24%), F^- (3.37%), SiO_2 (2.42%), SO_3 (2.21%), CO_2 (1.13%), Na_2O (0.92%), MgO (0.68%), Al_2O_3 (0.46%), Fe_2O_3 (0.36%), K_2O (0.04%) as well as trace amounts of several metals in the ppm range [14].

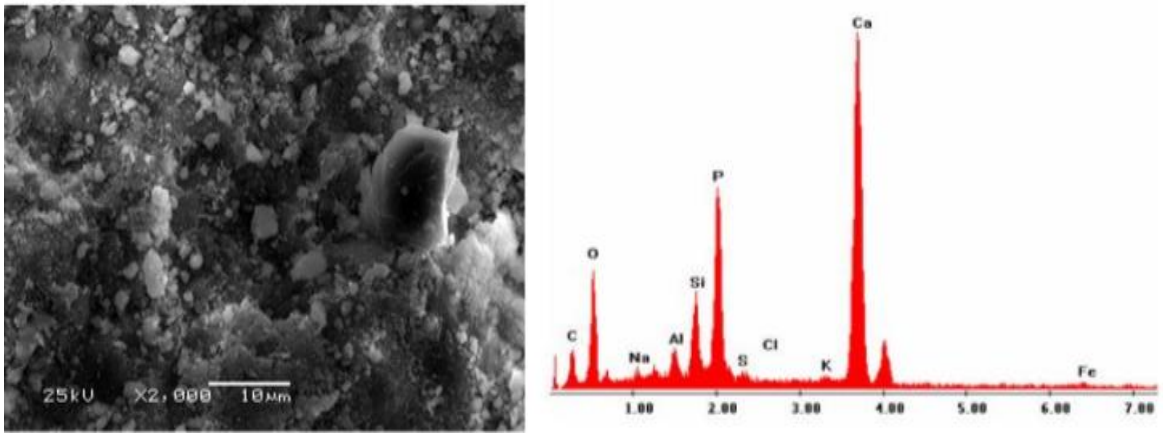

Figure 1. Electron micrograph of rock phosphate.

The crystal-chemical structure of the material closely resembles Matching that of fluoroapatite ($Ca_{10}(PO_4)_6F_2$), as verified through X-ray diffraction (as shown in Figure 2) and infrared emission spectroscopy (as depicted in Figure 3) [15]. The fluoroapatite framework is known for its high adaptability to substitutions and vacant positions. For instance, it allows for the substitution of Ca with elements such as Sr, Pb, Co, and Na, while PO_4 can be exchanged with AsO_4, VO_4, and SO_4, and F^- can be replaced by OH^- and Cl^-.

The natural phosphate material exhibits a relatively modest specific surface area, estimated at around 1 $m^2 \cdot g^{-1}$.

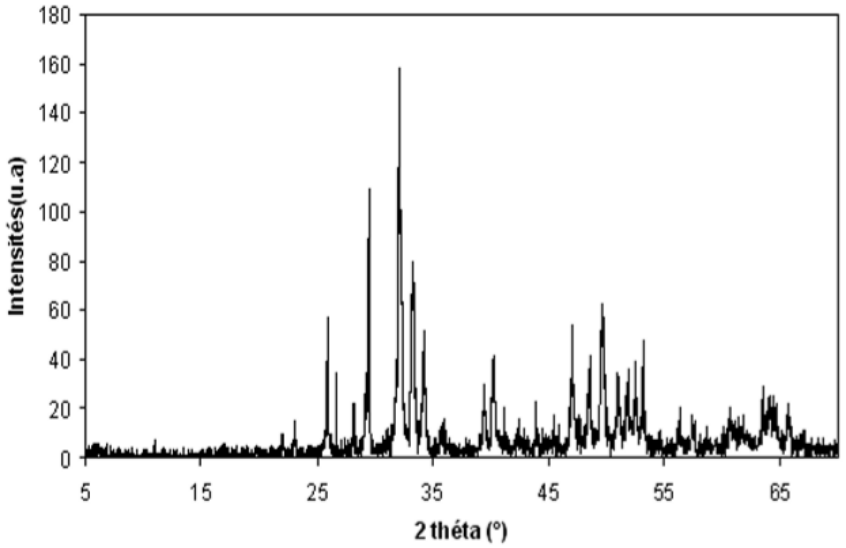

Figure 2. X-Ray diffraction spectrum of natural phosphate after treatment.

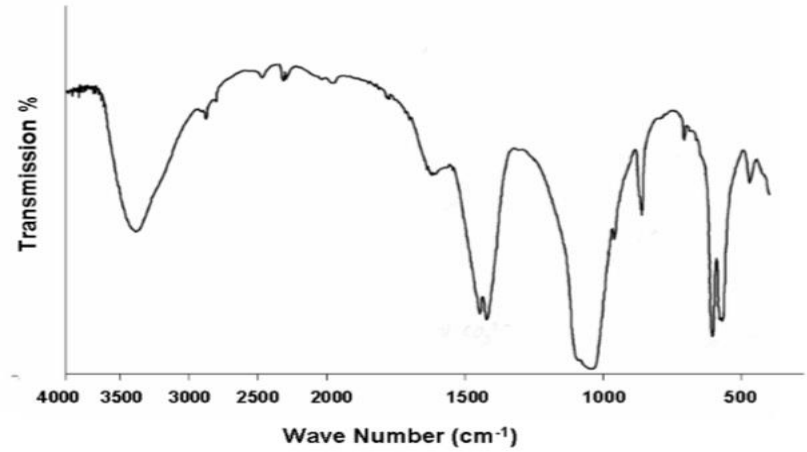

Figure 3. Infrared adsorption spectrum of natural phosphate treated at 900°C.

The synthesized molecules are the following:

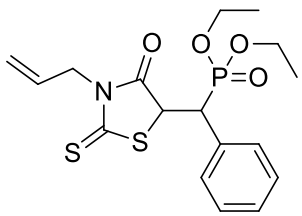

diethyl ((3-allyl-4-oxo-2-thioxothiazolidin-5-yl)(phenyl)methyl)phosphonate

Scheme 1. Molecule **A**.

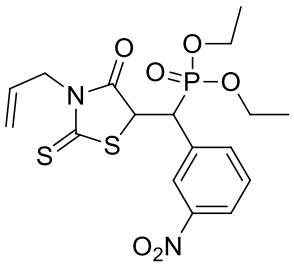

diethyl ((3-allyl-4-oxo-2-thioxothiazolidin-5-yl)(3-nitrophenyl)methyl)phosphonate

Scheme 2. Molecule **B**.

The Schemes above show that molecules **A** and **B** are different; that is, molecule **B** has a NO_2^- group in meta position of the phenyl.

3.2. Electrochemical studies of synthesized organic molecules

3.2.1. Molecule A

Figure 4 displays the cyclic voltammograms obtained from both CPE-NP electrodes (carbon paste electrode blended with natural phosphate in equal proportions) and CPE-NP modified with molecule **A**. The presence of molecule **A** in the CPE-NP electrode paste is evident from the emergence of multiple oxidation and reduction peaks. During the anodic scan, the voltammogram exhibits three sequential peaks, denoted as P1, P2, and P3, occurring at –0.8 V, 1 V, and 1.5 V, respectively. The initial oxidation (peak P1) is irreversible, followed by two reversible oxidations (peaks P2 and P3). In the cathodic scan, a fourth reduction peak (peak P4) is observed in the voltammogram.

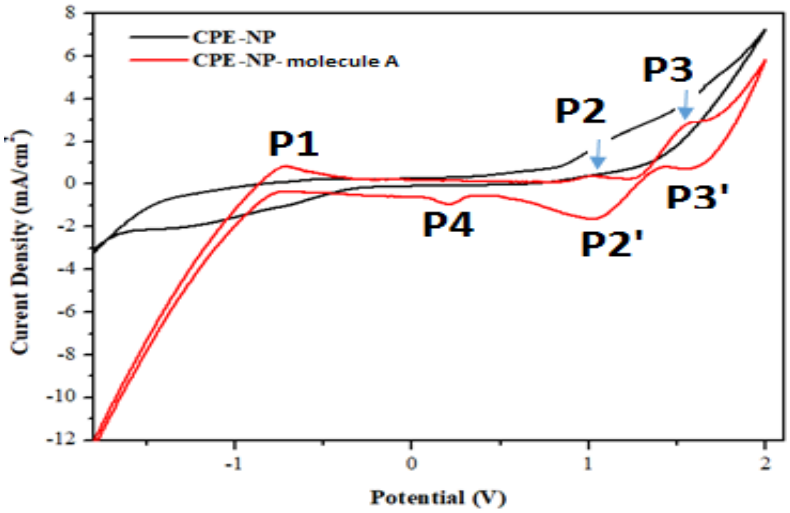

Figure 4. Cyclic voltammograms acquired for both CPE-NP and CPE-NP modified with molecule **A** in a 0.1 M Na_2SO_4 solution (pH=7), employing a scanning rate of 100 mV/s.

*3.2.2. Molecule **B***

When we changed aromatic aldehyde substitution by nitro in position meta, we obtain molecule **B**, whose cyclic voltammogram is shown in Figure 5. This voltammogram is characterized by the disappearance of the oxidation peak P2, which will be replaced by a reduction peak P5 that appears around –0.5 V. This suggests that the NO_2 function is characterized by the P5 reduction peak. The presence of molecule **B** in the paste modifies the shape of the electrochemical impedance curve, which is manifested by a succession of half loops (Figure 6) which appear at high frequencies and that can be attributed to the various redox reactions.

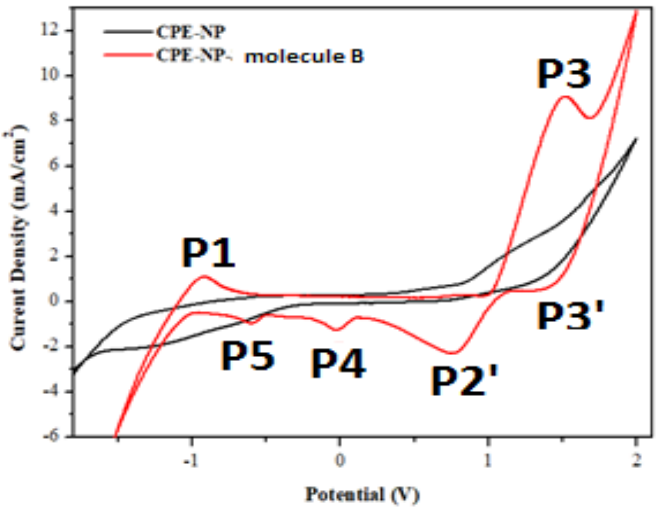

Figure 5. Cyclic voltammograms recorded for CPE-NP and CPE-NP modified with molecule **A** in a 0.1 M Na_2SO_4 solution at pH 7, utilizing a scanning rate of 100 mV/s.

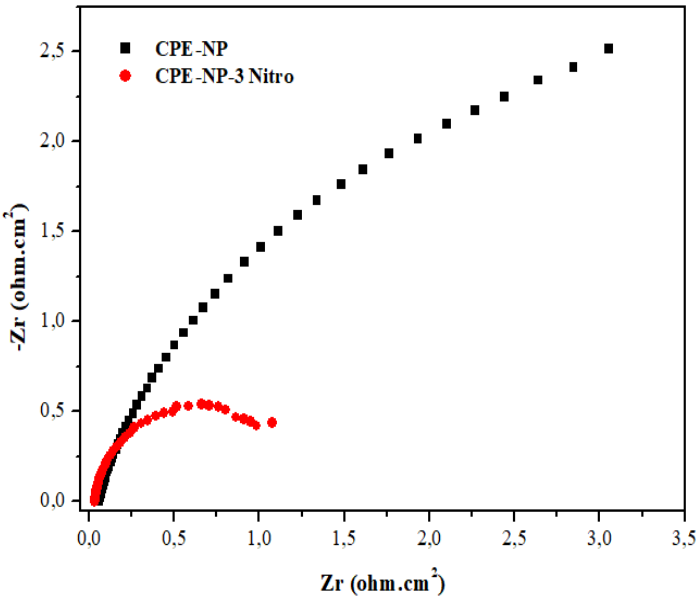

Figure 6. EIS for CPE-NP and CPE-NP-molecule **A** in 0.1 M Na_2SO_4 solution (pH=7).

3.3. Reduction of hydrogen peroxide

*3.3.1 Molecule **A***

Electrochemical impedance spectroscopy was employed to investigate the reduction of hydrogen peroxide on molecule **A**. (EIS). We present in Figure 7 The electrochemical impedance spectroscopy (EIS) plots captured at the CPE-NP-molecule **A** electrode's surface, respectively in the absence and presence of hydrogen peroxide. The curves have the shape of half loops, appear at high frequencies, having a diameter that aligns with the electron transfer resistance (R_t). We observed that when hydrogen peroxide (H_2O_2) is present the resistance decreases, this indicates that the reduction of hydrogen peroxide is more favorable when molecule **A** is present.

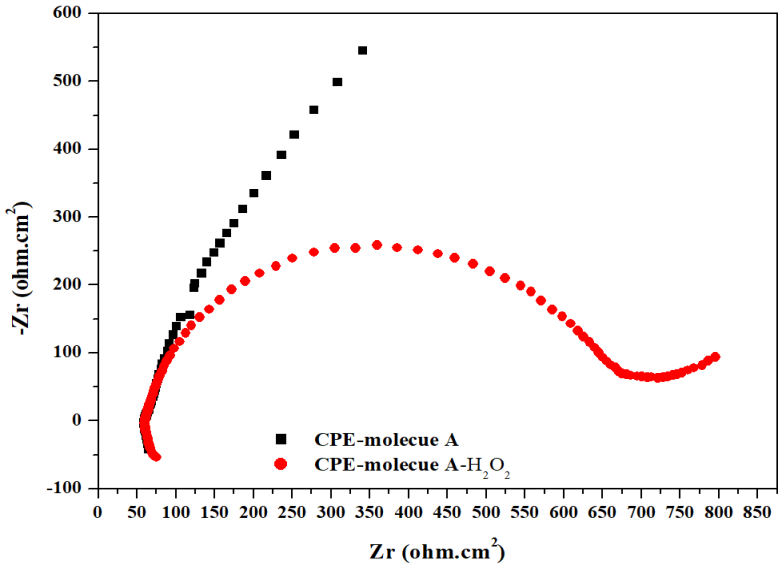

Figure 7. EIS data on CPE-NP and CPE-NP modified with molecule **B** in a 0.1 M Na_2SO_4 solution at pH 7.

The effect of the concentration of hydrogen peroxide on the shape of the EIS curves, at the surface of the CPE-NP-molecule **A** electrode, is presented in Figure 8. We note that the curves keep their shapes at different concentrations, suggesting that the H_2O_2 reduction mechanism is not affected by the concentration of hydrogen peroxide.

The electrochemical parameters deduced from the EIS curves, recorded on the surface of the CPE-NP-molecule **A** electrode, at different concentrations of H_2O_2, are summarized in Table 1.

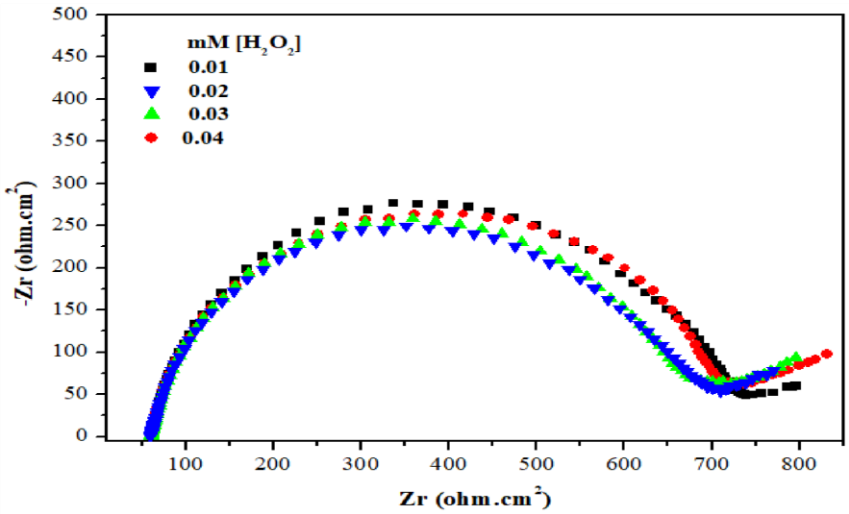

Figure 8. EIS for CPE-NP and CPE-NP-molecule **A** in 0.1 M $NaSO_4$ solution (pH = 7). Effect of H_2O_2 concentration.

Table 1. Electrochemical parameters deduced from EIS curves.

mM [H_2O_2]	Diameter, Ohm/cm^2	Correlation	R_1, Ohm/cm^2	R_2, Ohm/cm^2	R_t, Ohm/cm^2	C, µF/cm^2
0	3259	0.98	166.6	2833	2666.4	399.9
0.01	714.7	0.996	60.5	653.1	592.6	27.28
0.02	682.8	0.998	58.9	666.4	607.5	23.88
0.03	624.3	0.998	60.03	614.16	554.13	23.20
0.04	634.9	0.995	58.72	620.16	561.44	25.64

These electrochemical parameters show that the reduction of hydrogen peroxide takes place on the electrode CPE-NP modified with molecule **A**'s surface. The electron transfer resistance goes from 2666.4 Ohm/cm^2 in the absence of H_2O_2 to approximately 592.6 Ohm/cm^2 in the presence of hydrogen peroxide, which shows that this reaction is favorable on the elaborated electrode. The double layer capacity values indicate that the redox reaction is not significantly influenced by diffusion.

*3.3.2. Molecule **B***

The reduction of H_2O_2 at the CPE-NP-molecule **B** electrode's surface was also investigated using impedance spectroscopy (EIS) (Figure 9). It is noticeable that these curves exhibit a half-loop shape at high frequencies, indicating a faradaic reaction. Interestingly, the concentration of H_2O_2 does not alter the curve shape, suggesting that the reduction mechanism of hydrogen peroxide at the electrode's surface remains unaffected by its concentration.

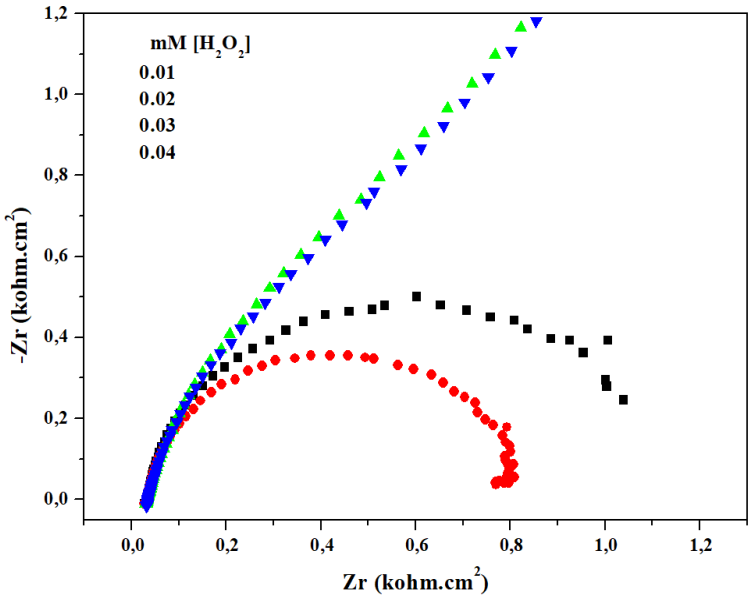

Figure 9. EIS data for both CPE-NP and CPE-NP-molecule **B** in a 0.1 M Na_2SO_4 solution at pH 7, while varying the concentration of H_2O_2.

The electrochemical parameters deduced from the EIS curves are gathered in Table 2. We find that the worth of the electron transfer resistance increased during the reduction of H_2O_2 at the surface of the CPE-NP-molecule **B** electrode, which suggests that molecule **B** does not promote the reduction of hydrogen peroxide.

Table 2. Electrochemical parameters deduced from EIS curves.

mM [H_2O_2]	Diameter, Ohm/cm^2	Correlation	R_1, Ohm/cm^2	R_2, Ohm/cm^2	R_t, Ohm/cm^2	C, µF/cm^2
0	1231	0.999	32.56	1219	1186.44	36.53
0.01	1123	0.996	26.34	1119	1092.66	35.53
0.02	791	0.999	32.75	787.3	754.55	31.93
0.03	4971	0.994	29.94	4695	4665.06	18.98
0.04	4863	0.991	31.90	4623	4591.10	17.21
0.05	5159	0.989	33.01	4878	4844.99	18.26
0.06	2981	0.997	32.26	2883	2849.74	15.45

3.4. Characterization by optical spectroscopy

The morphology of the elaborated electrodes (CPE, CPE-NP, CPR-NP-molecule **A** and CPE-NP-molecule **B**) was studied by optical microscopy (Figure 10). We note that the carbon paste electrode (CPE) has a compact and continuous surface. The presence of natural phosphate causes reliefs to appear, and sometimes agglomerations scattered over the entire surface; whereas, the addition of molecule **A** in the paste manifests itself in spherical clusters

deposited on the superficial surface. The same morphology is observed in the case of the CPE-NP-molecule **B** electrode, except that the organic clusters are larger.

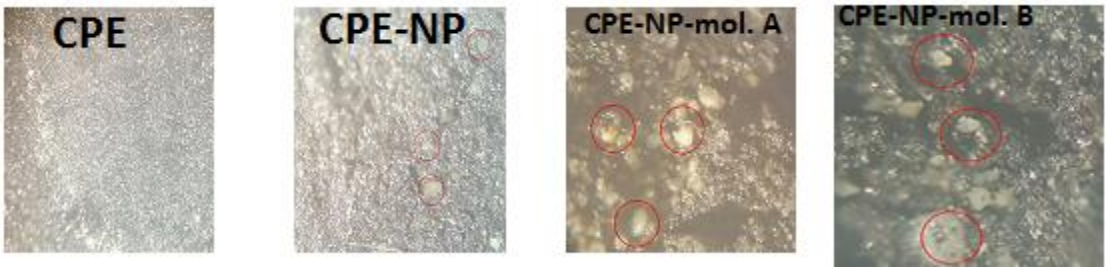

Figure 10. Images taken by optical microscopy of the elaborated electrodes.

3.5. Determination of the antioxidant power (PAO) of the molecules studied

$$\mathrm{PAO} = \frac{R_t^0 - R_t(H_2O_2)}{R_t^0} \cdot 100$$

With R_t^0 the electron transfer resistance deduced from the EIS curves in the absence of H_2O_2 and $R_t(H_2O_2)$ the electron transfer resistance drawn from the EIS curves during the reduction of hydrogen peroxide on the surface of the various elaborate electrodes. The results obtained are gathered in Table 3.

Table 3. Results of the antioxidant power of elaborated electrodes.

Electrode	**CPE-NP-molecule A**	**CPE-NP-molecule B**
ODP %	79	7

4. Conclusion

In this work, we developed paste electrodes from a mixture of graphite carbon and natural phosphate, modified by organic molecules. The purpose of This study aims to introduce a straightforward and efficient method for characterizing specific organic products. Cyclic voltammetry makes it possible to separate the properties of organic products, by the aspect of different oxidation and reduction peaks. The existence of NO_2 groups inside the backbone of organic molecule **A** is manifested by the disappearance of the 1 V oxidation peak (P2), and its replacement by a reduction peak around approximately –0.5 V (P5). These electrodes are also characterized by the hydrogen peroxide reduction reaction, which shows that the CPE-NP-molecule **A** electrode has a very high activity towards this reaction; whereas, the second electrode CPE-NP-molecule **B**, does not promote this reduction. In the same manner, the antioxidant power of the two molecules has been deduced. We find that molecule **A** has a remarkable antioxidant power compared to that of molecule **B**.

References

1. H. Gao, Y. Chen, X. Qi and W. Sun, Electrochemical deoxyribonucleic acid biosensor based on the self-assembly film with nanogold decorated on ionic liquid modified carbon paste electrode, *Anal. Chim. Acta*, 2011, **704**, no. 1–2, 133–138. doi: 10.1016/j.aca.2011.07.044
2. J. Wang, Nanoparticle-Based Electrochemical DNA Detection, *Anal. Chim. Acta*, 2003, **500**, no. 1–2, 247–257. doi: 10.1016/s0003-2670(03)00725-6
3. A.M. Pisoschi, A. Pop, F. Iordache, L. Stanca, L. Bilteanu and A.I. Serban, Antioxidant Determination with the Use of Carbon-Based Electrodes, *Chemosensors*, 2021, **9**, no. 4, 72. doi: 10.3390/chemosensors9040072
4. A. Chtaini, H.G. Valery, T.R. Ngono, H. Saâdane, M. Ennachete, M. Khouili, A. Hafid and L. Benoît, Evaluation of Carbon Paste Electrodes Modified with Organic Molecules for the Analysis of Heavy Metals by Square Wave Voltammetry, *Pharm. Anal. Acta*, 2013, **4**, no. 10, 1000271. doi: 10.4172/2153-2435.1000271
5. B. Wang, L. Bouffier, M. Demeunynck, P, Mailley, A. Roget, T. Livache and P. Dumy, New Acridone Derivatives for the Electrochemical DNA-hybridisation Labelling, *Bioelectrochemistry*, 2004, **63**, no. 1–2, 233–237. doi: 10.1016/j.bioelechem.2003.10.020
6. O. Estévez-Hernández, I. Naranjo-Rodríguez, J.L. Hidalgo-Hidalgo de Cisneros and E. Reguera. Evaluation of Carbon Paste Electrodes Modified With 1-furoylthioureas for the Analysis of Cadmium by Differential Pulse Anodic Stripping Voltammetry, *Sens. Actuators, B*, 2007, **123**, no. 1, 488–494. doi: 10.1016/j.snb.2006.09.030
7. K. Kalcher, Chemically Modified Carbon Paste Electrodes in Voltammetric Analysis, *Electroanalysis*, 1990, **2**, no. 6, 419–433. doi:10.1002/elan.1140020603
8. M.G. Paneli and A. Voulgaropoulos, Applications of Adsorptive Stripping Voltammetry in the Determination of Trace and Ultratrace Metals, *Electroanalysis*, 1993, **5**, no. 5–6, 355–373. doi: 10.1002/elan.1140050502
9. T. Hori and K.B. Sharpless, Selenium-Catalyzed Nonradical Chlorination of Olefins with N-Chlorosuccinimide, *J. Org. Chem.*, 1979, **44**, no. 23, 4204–4208. doi: 10.1021/jo01337a046
10. B. Hasimujiang and Z. Ruan, Electrochemical Synthesis of Organoselenium Compounds: A Graphical Review, *SynOpen*, 2023, **7**, no. 4, 511–520. doi: 10.1055/a-2184-8411
11. R.M. Kotkar and A.K. Srivastava, Voltammetric Determination of Para-aminobenzoic Acid Using Carbon Paste Electrode Modified with Macrocyclic Compounds, *Sens. Actuators, B*, 2006, **119**, no. 2, 524–530. doi: 10.1016/j.snb.2006.01.005
12. V. Stockhausen, J. Ghilane, P. Martin, G.T. Allard, H. Randriamahazaka and J.-C. Lacroix, Grafting Oligothiophenes on Surfaces by Diazonium Electroreduction: A Step toward Ultrathin Junction with Well-Defined Metal/Oligomer Interface, *J. Am. Chem. Soc.*, 2009, **131**, no. 41, 14920–14927. doi: 10.1021/ja9047009

13. R. Maallah, A. Moutcine and A. Chtaini, Bioelectrochemical Systems for Clean Environment, *J. Biosens. Bioelectron*., 2016, **7**, no. 4, 1000231. doi: 10.4172/2155-6210.1000231
14. R. Maallah and A. Chtaini Bacterial Electrode for the Oxidation and Detection of Phenol, *Pharm. Anal. Acta*, 2018, **9**, no. 3, 1000580. doi: 10.4172/2153-2435.1000580
15. M. Oubaouz, I. Smaini, R. Maallah, S. El Bahraoui, Y. Tahiri, A. Smaini, E. El Qouatli and A. Chtaini, Zinc Modified Carbon Paste Anode for Microbial Fuel Cells, *J. Xdian Univ*., 2022, **16**, no. 11, 539–548. doi: 10.37896/jxu16.11/058

♦ ♦ ♦